FEATURE ARTICLE

ChemComm
www.rsc.org/chemcomm

Squalene–hopene cyclase: catalytic mechanism and substrate recognition

Tsutomu Hoshino* and Tsutomu Sato

Department of Applied Biological Chemistry, Faculty of Agriculture, Niigata University, Ikarashi, Niigata 950-2181, Japan. E-mail: hoshitsu @agr.niigata-u.ac.jp

Received (in Cambridge, UK) 3rd October 2001, Accepted 9th November 2001
First published as an Advance Article on the web 17th January 2002

Rapid progress on the catalytic mechanism and substrate recognition by squalene–hopene cyclase, which has occurred only in the last several years, is reported. A series of site-directed mutation experiments and some squalene analogues have provided deep insight into the polycyclization mechanism and catalytic sites in conjunction with the information from X-ray crystal data.

Introduction

Over the last half-century, special attention has been paid to the cyclization mechanisms of squalene **1** or oxidosqualene **5** by organic chemists and biochemists.[1a,b] The enzymatic polycyclization reactions proceed with precise stereo- and regiospecificity to construct multi C–C bonds leading to a variety of triterpenoid carbocyclic skeletons including hopene **2** (from prokaryotic species), tetrahymanol (from Protozoa), lanosterol **6** (from yeast, fungi and animals), and a number of plant triterpenes such as cycloartenol, α- or β-amyrin, lupeol and so on.[1] To date, more than 80 different carbocyclic skeletons are known. Prokaryotic cyclase (SHC) converts squalene into the pentacyclic hopane skeleton. Eukaryotic cyclases (OSCs) mediate the catalytic reactions of (3*S*)-2,3-oxidosqualene into lanosterol or a variety of plant triterpene skeletons. These elegant polycyclization reactions involving multi-reaction steps are attained by a single enzyme. In the case of lanosterol formation, (3*S*)-2,3-oxidosqualene **5** first adopts a pre-organized chair–boat–chair conformation. Protonation of the epoxide ring then triggers a cascade of ring-forming reactions to protosterol cation **7** and a series of 1,2-shifts of hydride and methyl groups in an antiparallel manner leads to lanosterol **6** (Scheme 1b). Formation of the pentacyclic skeleton proceeds by adopting an all pre-chair conformation leading to C(22)-hopanyl cation **4**, which then undergoes a deprotonation from the terminal methyl group to give **2** or alternatively a nucleophilic attack by a water molecule to afford hopanol **3** (**2**:**3** = *ca.* 5:1), but such rearrangement reactions observed on lanosterol biosynthesis are not involved (Scheme 1a). The polycyclization pathways, which are shown in Scheme 1, have been believed for a long time, but the energetically disfavored anti-Markovnikov addition(s) is involved in their reaction mechanisms. Recent studies have uncovered that polycyclization reactions proceed *via* discrete and rigidly held carbocation intermediates and that ring enlargement reaction(s) is involved in the polycyclization cascades by SHCs and OSCs; the 5-membered C- and/or D-rings are formed according to the Markovnikov rule prior to the ring expansion into the corresponding anti-Markovnikov 6-membered C-and/or D rings of **2** and **6**.

Rapidly advancing technology in molecular biology has facilitated isolating the genes for triterpene synthases from numerous biological species. Poralla and coworkers reported in 1986 the characterization and partial purification protocol for the SHC from the thermoacidophilic bacterium *Alicyclobacillus acidocaldarius*[2] and its DNA sequence in 1992.[3] The cyclization mechanism mediated by SHCs is analogous to that by OSCs (Scheme 1), suggesting that the two cyclases SHCs and OSCs are closely related. Ourisson *et al*. proposed the idea that triterpenoid cyclases should have evolved from a common ancestor cyclase, *i.e*. a bacterial hopanoid synthase.[4] Later, several SHCs were cloned and sequenced.[5] *Candida albicans* lanosterol synthase was first sequenced in 1992.[6] Many OSCs were then cloned and sequenced;[7] a variety of triterpene synthases from plant sources were cloned, sequenced and expressed by Ebizuka and coworkers.[8] Comparison of the sequence similarities among all the known prokaryotic and eukaryotic cyclases permitted researchers to deduce the putative active sites responsible for the polycyclization reaction. Aromatic amino acids are unusually abundant in both SHCs and

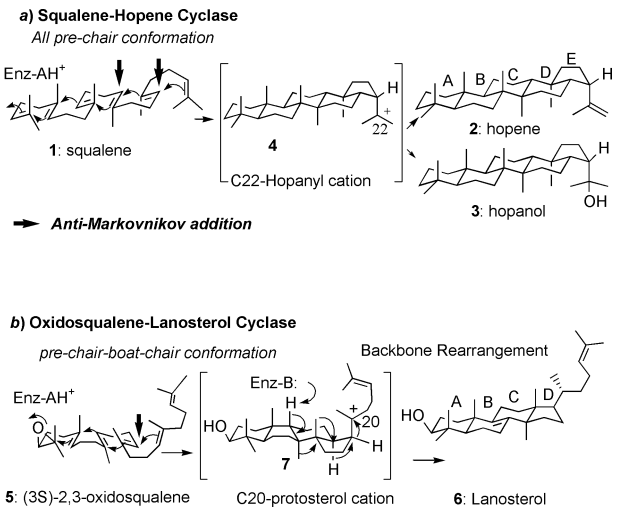

Scheme 1 Cyclization mechanisms by squalene–hopene (SHC) and (3*S*)-2,3-oxidosqualene–lanosterol synthases (OSC). According to this scheme, anti-Markovnikov addition(s), denoted by the symbol (→), occurs for both SHC and OSC.

Tsutomu Hoshino, born in 1951 in Japan, studied the chemistry of flower color variation (anthocyanin pigments) and prepared his doctoral thesis under the supervision of Professor Toshio Goto at Nagoya University. He began an academic career at Tokyo College of Pharmacy and then moved to Niigata University, where he has been full Professor of bioorganic chemistry since 1996. In 1987–1989, he joined the research group of Professor A. I. Scott, Texas A & M University, and was engaged in the biosynthetic studies of natural products. His current interest is focussed on the interdisciplinary field between organic chemistry and the enzymology of natural products with the aid of the protocols of molecular biology.

Tsutomu Sato, born in 1972, received his PhD degree in 2000 under the guidance of Professor T. Hoshino. He is now working as a research associate in this laboratory.

DOI: 10.1039/b108995c

OSCs. The following two characteristic motifs were noted in SHCs: one is the QW motif represented by the specific amino acid repeats $[(K/R)(G/A)X_{2-3}\ (F/Y/W)(L/I/V)_3X_3\ QX_{2-5}\ GXW]$, and the alternative is a DXDDTA motif. The number of QW motifs involved in bacterial SHCs depends on the strain: eight motifs for Gram-positive, but seven motifs for Gram-negative bacteria.[5] The QW motifs are also found in eukaryotes and the five motifs 1, 2, 3, 5c and 6 are commonly found in both SHCs and OSCs (Fig. 1).[7] The DXDDTA motif of prokaryotic SHCs corresponds to the VXDCTA motif of eukaryotic OSCs (Fig. 1).[7] Investigations of the SHC enzyme have been rapidly developed in the past several years. This remarkable progress is mainly due to successful overexpression in *Escherichia coli* and to stable properties at ambient temperature, because *A. acidocaldarius* is a kind of thermophilic bacterium, its optimum growth temperature being at 60 °C. These features have led to easy preparation of the homogeneously pure SHC using only two purification steps with the ionic exchange columns of DEAE and Mono Q at room temperature.[9] In 1997, Wendt *et al.* reported the X-ray analysis of *A. acidocaldarius* SHC, which is the first three-dimensional crystal structure among the many known triterpene synthases, revealing an α-helix-rich dumb-bell-shaped homodimer containing a large central cavity as the putative active site.[10] In contrast, OSCs are unstable and none of the OSCs has been overexpressed in *E. coli*; thus, no crystal structures of OSCs have been reported that can give valuable information for identifying the catalytic sites.

The excellent and extensively outlined reviews, regarding squalene and oxidosqualene cyclases, are now available.[1a,b] In this paper, we focus on the catalytic sites and the cyclization mechanism of the SHC, which were inferred from detailed kinetic analyses of many site-directed mutants and the structures of abortive cyclization products. The mutagenesis experiments have strongly been required to justify the hypothesis proposed based upon the X-ray analysis.[10] In addition, we outline here the key structural units in the substrate backbone for directing the polycyclization cascade. Site-directed mutants have given not only valuable information for identifying the active and/or catalytic sites but have also afforded unnatural natural triterpenes that have not been found before.

Two characteristic motifs

DXDDTA motif: initiation of polycyclization reaction

In 1996, Poralla's group reported the first mutagenesis experiments for the acidic residues of the D374XD376D377TA motif of *A. acidocaldarius* SHC.[11] Residues of D376 and D377 were mutated into Gln, Glu, Gly or Arg, and doubly into Gln, resulting in nearly quenching the SHC activity. They assumed that these residues are responsible for stabilizing the final carbocation intermediate **4** (Scheme 1a and 2), based on the result inferred from the affinity labeling experiment of a rat liver OSC using the suicide inhibitor, 29-methylidene-2,3-oxidosqualene (29-MOS, **94**); the VXDCTA motif of the OSC, equivalent to the DXDDTA motif of SHCs, was radiolabelled by ^{3}H-labelled 29-MOS.[12] In contrast, Corey *et al.* proposed the hypothesis, based on some point mutation experiments for *Saccharomyces cerevisiae* OSC, that the acidic proton of the Asp 456 residue in the VXDCTA motif may be responsible for the oxirane ring-opening reaction by protonation to initiate the polycyclization reaction, whereby Asp 456 acidity would be enhanced by the basic function of His 146.[13] According to the X-ray crystallographic data for the SHC complex with an inhibitor,[10] *N,N*-dimethyldodecylamine *N*-oxide (LDAO), Wendt *et al.* have proposed that the DX376DDTA motif is responsible for protonation on the terminal double bond to initiate the polycyclization and that H451 would enhance the acidity of D376 of this motif. Site-specific mutants of D377N or D377C in the DXD377DTA motif gave abortive cyclization product **8** (3-deoxyachilleol A, Fig. 2),[14a] strongly indicating that the DXDDTA motif is arranged in proximity to the initiation site in the active cavity and that D377 is likely to stabilize first cyclized carbocation intermediate **33** (Scheme 2).[14a] The mutation of D374 → N and/or D376 → N resulted in a complete loss of activity (Table 1),[14a] suggesting that the acidic proton(s) acted to initiate the polycyclization reaction. His451 was verified to function as a proton acceptor to enhance the acidity of D374 and/or D376 by the mutation experiments H → R and H → F;[14a] the cyclase activity of the H451F mutant was completely lost, while H451R retained the activity to some extent (Table 1). Our point mutation experiments validated

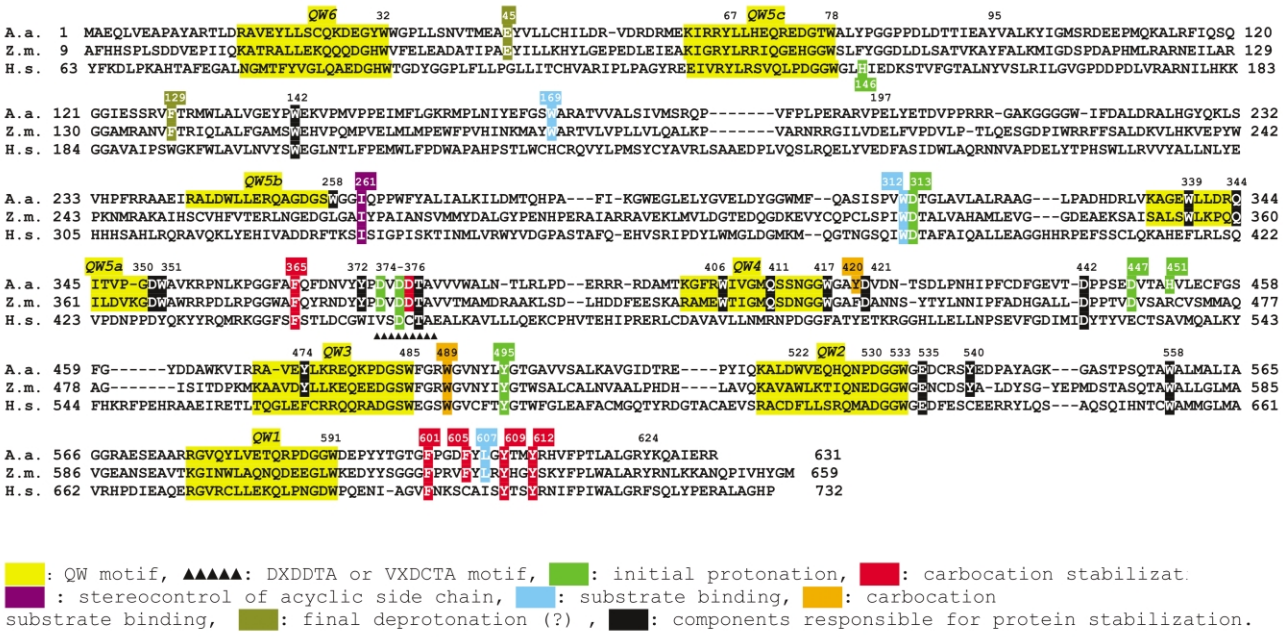

Fig. 1 Amino acid alignment of *Alicyclobacillus acidocaldarius* SHC (A.a.), *Zymomonas mobilis* SHC (Z.m.), *Homo sapiens* OSLC (H.s.). Two characteristic motifs (QW and DXDDTA) and the functions inferred from site-directed mutagenesis experiments are marked with colored boxes. The detailed functions of active sites, depicted here, are described in the text. None of the functions were found at positions 32, 67, 78, 95,197,485,522, 530, 533, 591 and 624.

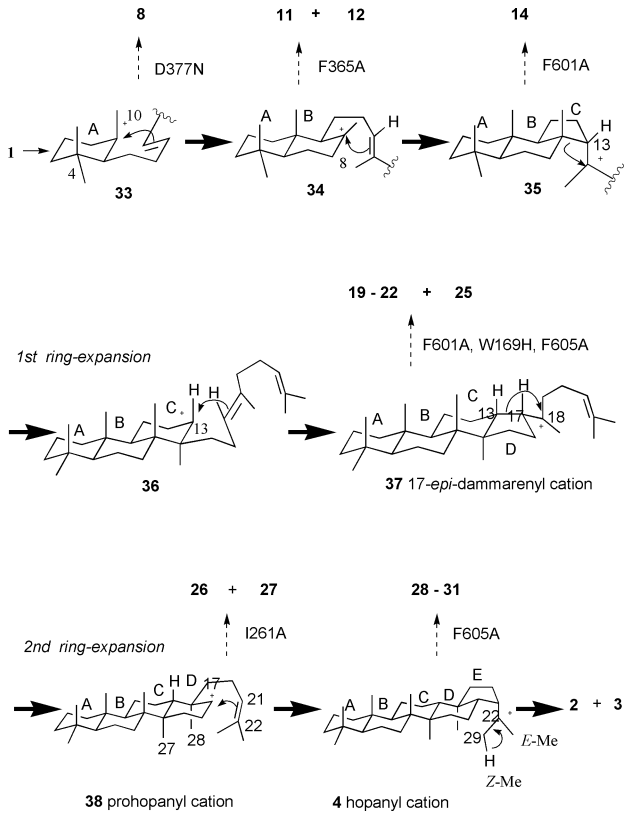

Scheme 2 The polycyclization pathway for hopene biosynthesis (⟶) and the carbocation intermediates accumulated by the mutated SHCs. The typical SHC mutants and their products are shown (**---**⟶). Products shown in Fig. 2 are obtained from each carbocation intermediate **33**–**38** and **4**.

Corey's hypothesis and are consistent with the proposal by X-ray analysis.[10] There may be a critical view for the stabilization of carbocation **33** by the D377 carboxylate anion, because a covalent bonding between them may be formed. Similar reports concerning the function of this motif have appeared.[14b,c] The wild-type SHC is able to convert (3*R*)- and (3*S*)-oxidosqualenes into 3α- and 3β-hydroxyhopene, respectively. Achilleol A (3-hydroxy **8**),[15] isolated from *Achillea odorata* L., was successfully prepared by incubating a racemic mixture of **5** with a single mutant D377N or D377C[14a] or with a triple mutant D377C/V380E/V381A.[14c] The residues V380 and V381 are also highly conserved among the known SHCs.[5] It was also suggested that the residues of D313 and D447 may facilitate initiation of the cyclization reaction (Table 1 and Fig. 3).[14a]

QW motif: reinforcement of the protein structure

W. S. Johnson proposed the concept of the negative point charges for the cyclization mechanism by OSCs; negatively charged ions included in OSCs are arranged in the enzyme cavity so as to stabilize the intermediary carbocations formed during the polycyclization reaction, leading to the acceleration of the polycyclization reaction.[16] Dougherty also proposed the idea that cation-π interaction is operative for the polycyclization reactions.[17] Based upon unusual richness of the aromatic amino acids and the repeated amino acid alignments of the QW motif, Poralla suggested that QW motifs may act to stabilize the transient carbocationic intermediates.[18] However, the X-ray analysis of the SHC showed that the QW motifs, which share two types of secondary structure, *i.e.*, α-barrel helices and a stacking structure of Trp with Glu, are arranged at the protein surface area; thus the motifs cannot interact with the substrate. Wendt *et al.* suggested that the motifs are responsible for reinforcement of the protein structure against an unusually high energy 200 KJ mol^{-1}, released during the process of pentacyclic ring formation from acyclic **1**.[10a] Site-directed mutations targeted at the 8 QW motifs involved in *A. acidocaldarius* SHC demonstrated that the motifs 4, 5a and 5b are responsible for stabilizing the protein structure against thermal denaturation.[19] The mutations of aromatic Trp into aliphatic amino acids such as Val, Leu, or Ala and those of Glu into Gly, targeted at QW motifs 4, 5a and 5b specifically present in SHCs, afforded a significantly lower temperature for the optimum catalysis.[19] Before the X-ray analysis was published, we had proposed in our first *in vitro* mutagenesis paper that W351 included in QW motif 5a was an active residue.[9] This was inferred from the kinetic results measured only at 60 °C,[9] *i.e.*, at the catalytic optimum temperature of the wild-type, where the cyclase activity of the mutant W351L was completely quenched, allowing us to propose that W351 was an active residue.[9] However, at temperatures less than 40 °C, the specific activity of the mutant was indistinguishable from that of the wild-type; the catalytic optimum temperature of the mutant was found at 49 °C.[19] Thus, reinforcement against thermal denaturation could be proposed for the function of the three QW motifs 4, 5a and 5b.[19] However, in spite of extensive mutation experiments, we have failed to assign any function for the other five motifs 1, 2, 3, 5c and 6,[19] which are commonly found in the families of both prokaryotic SHCs and eukaryotic OSCs; no change was observed in the optimal temperatures and the catalytic activity for the mutated SHCs targeted at their motifs.[19] Recent investigation of mutant Y474A, situated at QW 3, showed that this motif also reinforces the protein structure (Fig. 1).[20] Alterations of some Asp residues into Asn also caused a decrease in the catalytic optimum temperature (Fig. 1).

Aromatic amino acid residues crucial for the catalysis

As described above, a cation-π interaction concept has been proposed for stabilizing the transient carbocation intermediates.[17] Based on the information from both X-ray data and homologous alignment (Fig. 1), the three Phe residues of F365, F601 and F605 were mutated into aliphatic amino acids to address the function of the aromatic π-electrons. F365 and F601 are highly conserved among the prokaryotic and eukaryotic species. F605 is conserved in all the prokaryotic SHCs, which form the pentacyclic hopene skeleton, but not in lanosterol synthase forming a tetracyclic skeleton.

The incubation of **1** with the cell-free homogenates of the mutant F365A[21] afforded bicyclic compounds **11** and **12** (Fig. 2) in large quantity without completion of the polycyclization reaction, indicating that the F365 is placed on bicyclic carbocation **34**, which is stabilized *via* the interaction between the intermediary cation and the π-electrons of F365. Based upon the presumption that the greater π-electron density, the faster cyclization reaction, the mutants F365Y and F365W were constructed. The π-electron density increases in the following order: F < Y < W. The mutant F365Y completed the polycyclization reaction leading to final product **2** without any abortive cyclization product having been accumulated and exhibited a remarkable increase in the reaction rate at low temperatures (10–50 °C). The mutant F365Y produced **2** even at a temperature as low as 10 °C, where the wild-type SHC has no activity. The kinetic data of the F365Y are shown in Table 1. The K_m increased 30-fold (looser binding), whereas k_{cat} remarkably increased 41-fold (acceleration of reaction rate), compared with those of the native SHC. The significantly increased reaction rate (k_{cat}) by F365Y strongly suggests that cation-π interaction is operative for the polycyclization reaction, in spite of the occurrence of local changes at the active center due to the introduction of bulkier Tyr (larger K_m). The bulkiest Trp mutant had no activity (Table 1). This may be explained by the assumption that the binding of **1** with the Trp mutant was severely disturbed due to the introduction of the large steric bulk size of Trp, thus leading to little function of

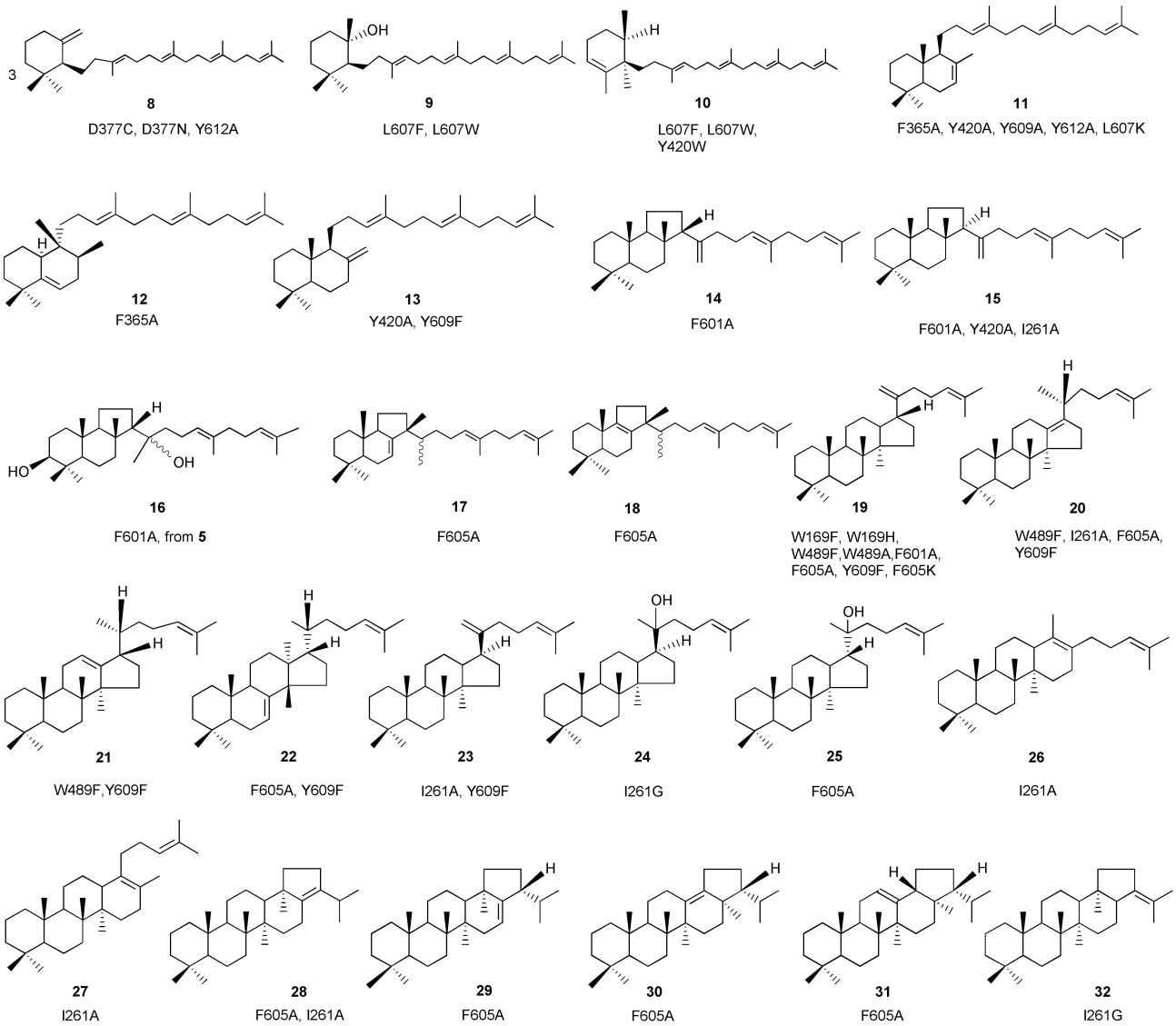

Fig. 2 Cyclization products obtained by the mutated *A. acidocaldarius* SHCs. Compound **16** was obtained by incubation of **5** with the mutant F601A.

cation-π interaction for the catalysis, despite the aromatic π-electron density being highly increased.

The mutant F601A[14b,22b] gave one tetracycle **19** and two tricycles **14** and **15** along with final products **2** and **3**. Isolation of tricyclic **14** and tetracyclic **19** has allowed us to propose that the ring expansion process forming a 5- to 6-membered ring occurs with respect to the 6-membered C- and D-ring formation of **2** (Scheme 2).[22a,b] Suggestions regarding the ring-D expansion from the 5-membered intermediate was also given by other workers,[22c] based upon the isolation of tetracyclic **19**–**23** in very small amounts (< 1%) by the native SHC. Both C- and D-ring expansion processes were further verified by the successful trappings of tri- **35** and tetracyclic intermediates **37** (Scheme 2) in very high yields.[22a,b] A highly nucleophilic hydroxy group of truncated analogue **39** (C-22 OH) could attack at C-14 of **40**, resulting in the formation of **41** having the tetrahydrofuran ring.[22b] The discrete C-20 cation of **47** was also trapped by analogue **46** (C-27 OH) to give **48** (see Scheme 3). These results indicate that intermediates **40** and **47** have a significantly longer lifetime prior to the ring expansion and further cyclization. However, no production of **42** and **50** was found in the incubation mixture by the wild-type SHC, further suggesting that the cyclization does not proceed in an all pre-chair conformation such as that shown in Scheme 1, which leads to anti-Markovnikov additions. Thus, the polycyclization reaction proceeds *via* ring expansion processes from the thermodynamically favored 5-membered **35** and **37** to the 6-membered C/D-rings (**36**, **38**), as shown in Scheme 2. The computational studies suggest that the most favourable placement of the aromatic ring on the secondary cation may facilitate the ring expansion reaction from the thermodynamically favourable tertiary cation.[23] The folding conformation of **1** leading to carbocation intermediates **35** and **37** was discussed in detail from the aspect of steric repulsion by 1,3-diaxial interaction.[22a,b] Our recent experiments using C30 analog **43**, with the same carbon number as **1**, showed that **45** having a 6,6,5-fused tricyclic ring system also was produced *via* intermediate **44** in a high yield,[24] further supporting the involvement of the ring expansion process in hopene biosynthesis. It is noticeable that the stereochemistry of the biosynthetic intermediates must have 13β-H in the 6,6,5-fused tricyclic and 17β-H in the 6,6,6,5-fused tetracyclic ring systems, because none of the stereoisomers of **41**, **45** and **48** having α-H orientation at C(13) and at C(17) were detected in the reaction mixtures by the native SHC.

The F605A mutant afforded many triterpenes up to 12, consisting of 6,6,5-fused tri- **17** and **18**, 6,6,6,5-fused tetra- **19**, **20**, **22** and **25**, and 6,6,6,6,5-fused pentacyclic skeletons **28**, **29**, **30** and **31**,[25] but the quantities of these abortive cyclization products produced by the mutants F605Y and F605W were negligible. The enhanced cyclization rate by the Tyr and Trp mutants (Table 1), compared to the wild-type, indicated that the

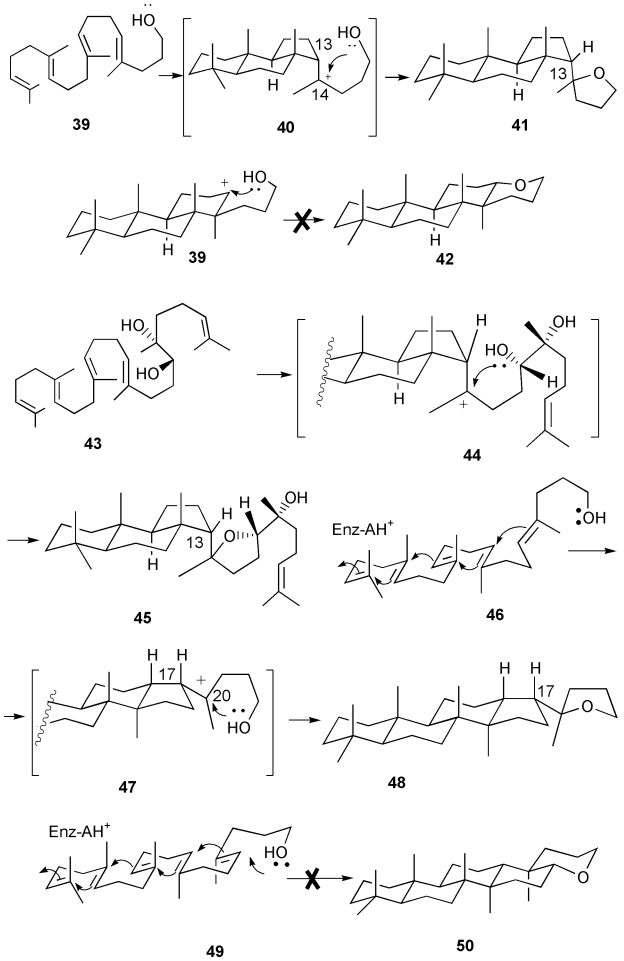

Scheme 3 Trapping of 6,6,5-fused tricyclic and 6,6,6,5-fused tetracyclic intermediary carbocations by incubating squalene analogues having a highly nucleophilic hydroxy group with the native SHC.

F605 residue may facilitate the ring expansion **37** → **38** as a result of the stabilization of the secondary cation **38** and also may stabilize **4**, possibly *via* cation-π interaction.

All the other aromatic amino acids conserved in the known SHCs have been mutated.[20] Accumulation of bicyclic **11** by mutant Y609A suggests that Y609 is arranged near to the position of bicyclic cation **34** in the enzyme cavity (Fig. 3). The production of bicyclic **11** and **12** was also observed for mutant F365. However, the yields of the bicyclic compounds were different. The higher yield of 96% for **11** and **12** by F365A, than that of *ca*. 50% by Y609A, suggests that the carbocation stabilization of **34** may have been achieved mainly by the π-electrons of F365 with the aid of those of Y609. When the phenolic hydroxy group is missing (mutant Y609F), the cyclization cascade proceeds toward tetracyclic intermediate **37**,[26b] suggesting that a perturbation around C-8 and/or lowering of the π-electron density is not significant on mutant Y609F. However, mutant Y609A had no π-electrons and underwent marked perturbation around the active site, thus ending polycyclization at the bicyclic reaction stage. Mutant Y612A gave monocyclic **8** (2.2%) and bicyclic **11** (5.6%),[20] the yields being low, compared to those of D377 and F365: 90% of **8** for D377C, and 96% of **11** and **12** for F365A. Y612 may intensify each function of both D377 and F365, possibly by placing D377 and F365 at positions sufficiently favorable for stabilizing cations **33** and **34** (Fig. 3). The loss of π-electrons and the phenolic hydroxy group in mutant Y612A could not amplify the negative charge of D377 and the π-electron density of F365, thus resulting in a slower reaction rate (Table 1). The mutant Y495A gave little change in K_m value (Table 1) and no abortive cyclization product, suggesting that little perturbation

Table 1 Kinetic data for catalytic sites of the mutated and native SHCs.[9,14a,19,20,21,22a,22b,25,27,29] Incubations were done at the temperatures where no thermal denaturation occurs

	K_m/μM	k_{cat}/ min^{-1}	k_{cat}/K_m	Relative activity	Optimal Temp. (°C)
	Measured at 60 °C and pH 6.0 for 60 min				
Wild-type	16.7	289	17.3	100	60
D313N	16.1	28.7	1.78	10.3	60
D374→E, I, V, N,	—[a]	—	—	0	—
D376N	—	—	—	0	—
D377→C, N	—	—	—	0	—
D447N	12.1	9.3	0.77	4.5	65
	Measured at 30 °C and pH 6.0 for 60 min				
Wild-type	16.7	6.43	0.385	100	60
H451F	—	—	—	0	—
H451R	16.9	1.22	0.072	18.8	60
W169V	—	—	—	0	—
W169F[b]	276	5.43	0.173	5.2	45
W169H	280	2.36	0.00843	2.2	45
W312L	—	—	—	0	55
W312F[b]	55.1	5.86	0.106	27.6	55
F365A	—	—	—	0	55
F365Y	502	266	0.53	137.7	25–55
F365W	—	—	—	0	55
W489L	—	—	—	0	—
W489F[b]	91.9	0.929	10.1	2.6	53
F601A[c]	1220	55.8	0.0457	11.9	30-45
F601Y[c]	179	7.00	0.0391	10.2	55
F601W[c]	287	12.9	0.0449	11.7	50
F605A	47.9	6.07	0.127	33.0	55
F605Y	22.6	14.4	0.637	165.5	55
F605W	23.2	22.9	0.987	256.4	45–55
I261A	20.5	3.14	0.153	39.7	60
I261V	18.9	6.57	0.348	90.4	60
	Measured at 45 °C and pH 6.0 for 60 min				
Wild-type	16.2	51.8	3.19	100	60
F129A	18.5	13.7	0.741	23.2	60
Y420A	90.9	1.64	0.18	5.6	55
Y495A	17.2	28.7	1.67	52.4	60
Y609A	—	—	—	0	60
Y612A	13.3	24.4	1.83	57.4	60

[a] The symbol (—) shows nearly complete loss of the SHC activity. [b] Compared with the kinetic data of the wild-type, mutants W169F and W312F had increased K_ms 17-fold and 3.3-fold, respectively, but the V_{max}s remained unchanged, suggesting that both W169 and W312 would bind to **1** rather than stabilizing the carbocation *via* cation-π interaction. W489F had a 5.5-fold larger K_m, but V_{max} was only 14% of the wild-type, implying that W489 may exhibit both binding and cation stabilization. See Fig. 3. These results also suggest that the higher the π-electron density, the greater is the affinity for **1**. [c] F601A showed a significantly higher reaction rate in the low temperature region, compared with the wild-type, the reason not being clear at the present time. In the case of oxidosqualene substrate **5**, V_{max}s of F601Y and F601W greatly increased (unpublished results), suggesting cation-π interaction for the function of F601.

occurred by the mutation and that the residue Y495 arranges near the initiation site inside the active enzyme cavity. It has been pointed out that the phenolic hydroxy group of Y495 may further enhance the D376 acidity for initial protonation through a hydrogen-bond with a water molecule (Fig. 3).[1b,26b] Mutant Y495F had no enzyme activity, and it was thus inferred that the phenolic hydroxy group was crucial for catalysis.[26b] However, the Y495A mutant still retained 52% of the activity of the wild-type (Table 1), despite the hydrogen bond being missing like the Phe mutant.[20]

Steric bulk size of active sites: stereo-control and optimal folding

It is significant to address the question of how fine stereochemical control can be attained by the squalene cyclase, leading to the construction of only one stereoisomer **2** despite 2^9 isomers being possible (nine chiral centers in **2**). Evidence has

been obtained that the steric bulk size of the amino acid residue controls the stereochemical destiny; the replacement of Ile by the less bulky Ala or Gly at the 261 position resulted in the accumulation of **15**, **20**, **23**, **24**, **26**, **27**, **28** and **32** (Fig. 2), which possess the stereochemistry of α-configuration for 13H and 17H of tri- and tetracyclic skeletons.[27] Interestingly, the dammarenyl cation, having 17α-H orientation opposed to that of **37** (17-*epi*-dammarenyl cation), a biosynthetic intermediate of some plant triterpenes,[1a] was formed by this single amino acid substitution. Products derived from true intermediates of tricyclic **35** and tetracyclic **37**, which have 13β- and 17β-H orientation, respectively, were found in no detectable amount in the incubation mixtures with the Ala and Gly mutants. On the other hand, the I261V mutant afforded no abortive cyclization product and the kinetic data were almost the same as that of the wild-type SHC (Table 1). These results strongly indicate that the steric bulk size of a given amino acid of the cyclase determines the stereochemical destiny during the polycyclization cascade. In addition, two novel triterpenes **26** and **27** have been found by the Ala and the Gly mutants, which are named prohopene B and A, respectively, further indicating the presence of prohopanyl cation **38** as the intermediary cation; no evidence for the involvement of intermediate **38** had been given before this point mutation experiment appeared. We can now illustrate the complete cyclization mechanism leading to the hopene skeleton from squalene as shown in Scheme 2. Only the 6,6,6-fused tricyclic intermediate **36** has not been trapped in spite of extensive mutagenesis experiments. The SHC activity is inhibited by aza-squalene derivatives, which can mimic the high energy transient carbocations produced during the polycyclization reaction,[28] further supporting that the polycyclization for hopene biosynthesis proceeds *via* rigidly held carbocation intermediates such as shown in Scheme 2, but not in a concerted manner.

Another example was recently found in which alteration of the bulk size of the active components dramatically influences the cyclization pathway. Compound **10** could be produced by a single amino acid substitution of Y420 or L607 with bulkier W or F.[29] Taking into consideration the stereochemistry of the monocyclic ring in **10**, **1** had been folded in a pre-boat form, but not in the usual pre-chair form; the larger bulk size of W or F may have induced a constrained boat form (see **76** and **77**). Compound **10** has a novel triterpene skeleton. Recent investigations of eukaryotic OSCs, carried out by Matsuda and coworkers, also indicated that the steric bulk size influences the polycyclization cascade and deprotonation reaction, which was demonstrated by altering the bulky residue Ile into the less bulky Ala or Gly.[30a,b] Steric bulk size at active or catalytic sites may be one of the important factors which confer the structural diversity of the triterpenes and the stereochemical specificity for the formation of a given triterpene skeleton. To ascertain this, numerous examples should be given by a series of mutagenesis experiments.

Fig. 2 summarizes the structures of all the triterpenes produced by the mutated SHCs, which have been isolated by us and Poralla's group.[14b,26] A variety of triterpene skeletons were produced, among which **10**, **12**, **26** and **27** have unprecedented triterpene skeletons.

Fig. 3 depicts the arrangements and the functions of the crucial amino acids inside the enzyme cavity, which are responsible for the molecular recognition and for the catalysis. The mutations of W169, W312 and W489 into aliphatic Leu or Val resulted in no cyclase activity. Replacing them by aromatic Phe enabled the recovery of enzyme activity, but with decreased activities (Table 1). On prolonged incubation, W312L gave no enzymic product, verifying that the residue is located close to the initiation site. On the other hand, W169F and W169H afforded tetracyclic **19** together with **2** and **3**, suggesting that these residues are located close to the D-ring formation sites (Fig. 3). The K_ms of W169F and W312F remarkably increased, but the V_{max}s remained unchanged (Table 1), indicating that the residues of W312 and W169 may function for binding with **1**

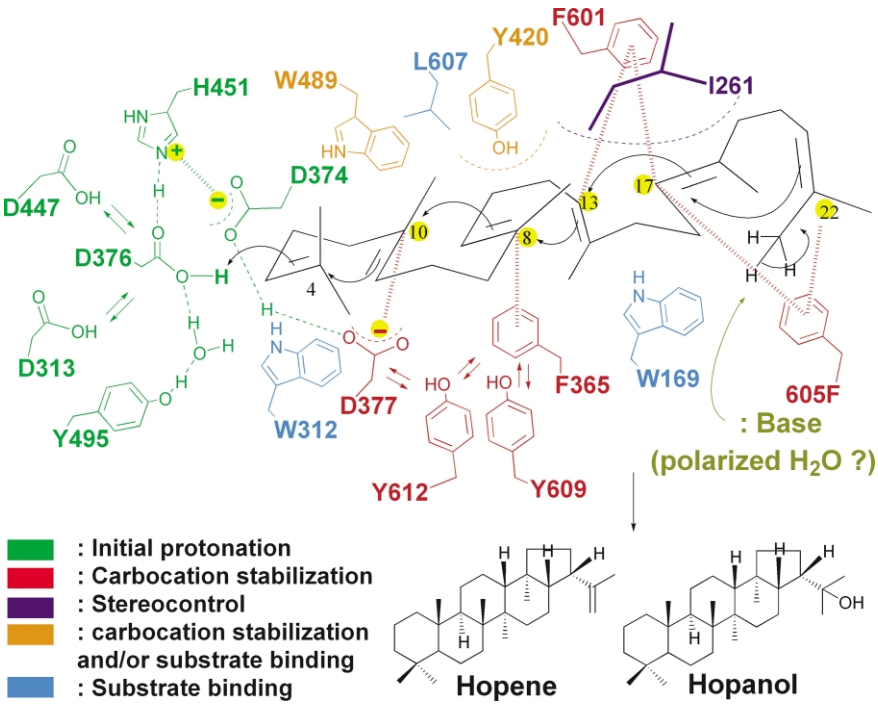

Fig. 3 The placements and functions of crucial amino acids inside the central cavity, proposed based upon the kinetic data (Table 1) and structures of prematurely quenched products (Fig. 2) in conjunction with X-ray information.[10] The numbering on the squalene backbone is according to hopene numbering. Y612 and Y609 may function to place D377 and F365 at the correct positions in the enzyme cavity and to enrich the negative charge of D377 and the π-electrons of F365, so that D377 and F365 can effectively stabilize their carbocationic intermediates **33** and **34**. D313 and D447 may function to enhance the D376 acidity, but the mechanism(s) is not clear. The symbol shows the presence of such interaction(s) among D313, D447, D376, F365, Y609 and Y612. W312 is likely to arrest the terminal isopropylidene methyl group(s), based on the kinetic results.[19] The major function of Y420 is ascribed to be the stabilization of the intermediary cation **34**, but Y420 may have a stereo-control function which directs the cyclization pathway, because **15** was produced from an erroneous intermediate having 13α-H opposed to 13β-H of **35**.

rather than cation-π interaction. This is in contradiction with the proposal by Wendt *et al*., who assigned the stabilization of the C-4 cation (hopene numbering) and the C-13 cation of **36** *via* cation-π interaction for W312 and W169, respectively.[1b,10b] Thus, it can be inferred that aromatic amino acids are not only responsible for the cation-π interaction but also can function in the binding with the substrate. W489 may have the functions of both cation stabilization and substrate binding, based on the kinetic analysis of W89F mutant (Table 1). The mutants W489F produced only tetracyclic **19**–**21** other than **2**, suggesting the positioning around the D-ring formation site. However, the X-ray analysis shows that the residue is situated close to the C-10 cation of **33**,[10] thus Wendt *et al*. proposed that W489 may work for stabilizing the cation through cation-π interaction.[10b] The reason why tetracyclic **19**–**21** was produced is not clear, despite W489 being positioned around the C-10 cation of **33**.[1b] One plausible answer may be as follows. When the Trp was replaced by the smaller bulk size of Phe, the cyclization reaction may further have proceeded up to the relatively stable tetracyclic carbocation intermediate **37** without quenching at the monocyclic stage, although W489 is situated close to C-10 of **33**. This idea would be consistent with the finding that significantly high production of tetracyclic products **19**–**23** occurred by the Y609F mutant (Fig. 2), [26b] despite Y609 being positioned around the C-8 cation of **34**. The function of Y420 is likely to be assigned for stabilization of the C-8 cation of **34** (Table 1),[26,29] because Y420A[26a,c] and Y420G[29] afforded bicyclic **11** and **13** in a high yield. In addition to the bicyclic products, tricyclic **15**, having the 13α-H opposed to that of true intermediate **35**, was concomitantly produced in a small amount, suggesting that Y420 may have an additional function for the stereochemical control of the polycyclization cascade. The function of E45[10,14c] has been presumed to be responsible for the final deprotonation reaction, but that of F129[20] still remains unclear.

Key structural units in substrates for molecular recognition and for correct folding

In contrast to the extensive studies on lanosterol synthase using substrate analogues,[1a,b] little is known of substrate recognition by the SHC, though a few reports have appeared.[1,28] The cyclization mechanisms of the two cyclases are similar. First, we describe the important findings for lanosterol synthases. Next, we discuss the structural elements and molecular recognition of the squalene substrate with the SHC in comparison with those of lanosterol synthases.

C-ring expansion and the importance of the bulk size at C(10) and C(15) in lanosterol biosynthesis

As described above, ring expansion reactions occur twice in hopene biosynthesis (Scheme 2). Previously, Corey *et al*. proposed that the ring expansion process from **51** to **52** is involved during lanosterol biosynthesis (Scheme 4),[31] based upon the isolation of the 6,6,5-fused tricyclic A/B/C-ring system **55**–**57** and **60** having a chair–boat–chair structure, which is obtained from the incubation of C20-truncated analogue **53**[31a] and 20-oxa analogue **58**[31b] (Scheme 4), respectively. The tricyclic compounds having a five-membered C-ring have also been isolated from the 18(*Z*)-2,3-oxidosqualene analogue by Krief *et al*.[32] In addition, Corey *et al*. have reported a very interesting study; analogue **61** lacking two methyl groups at both C(10) and C(15) afforded unusual product **64** having the 6,6,5-fused A/B/C tricyclic ring system, which is further linked with a 4-membred ring, where the B-ring has a chair structure. This result suggests that the cyclization had proceeded in a pre-organized chair–*chair*–boat (A/*B*/C) conformation (Scheme 5), which is in contrast to the usual folding of **5** into the chair–boat–chair conformation by lanosterol synthase (Schemes 1 and 4).[33] Replacement of the methyl group at C(15) with hydrogen led to the normal

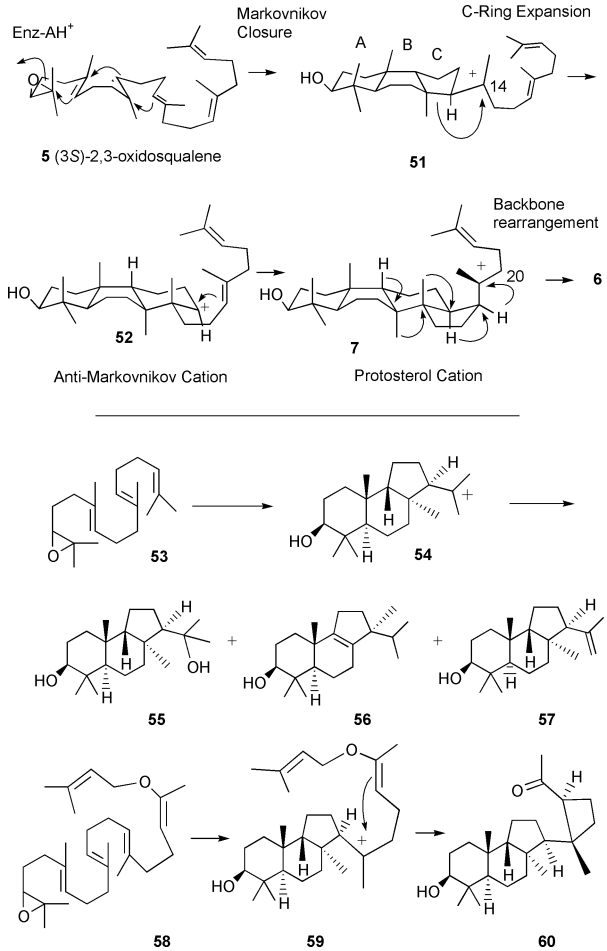

Scheme 4 The cyclization pathway in lanosterol biosynthesis (top) and the trapping of 6,6,5-fused tricyclic A/B/C-ring system, where the B-ring adopts a boat form, by using 2,3-oxidosqualene analogues (bottom).

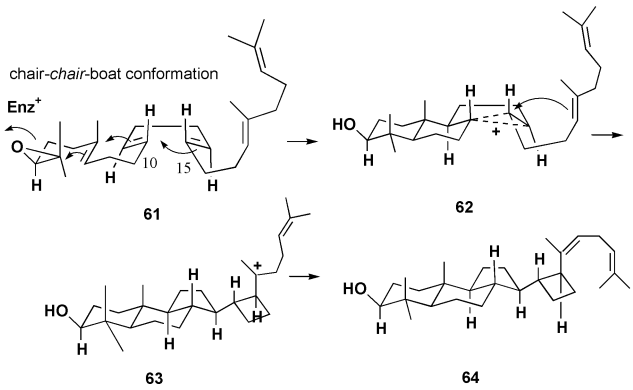

Scheme 5 Chair–chair–boat conformation of 10,15-bisdesmethyl-2,3-oxidosqualene, folded by lanosterol synthase, in contrast to the usual chair–boat–chair conformation.

cyclization having a chair–boat–chair structure.[34] These findings strongly indicated that the methyl group at C(10) is crucial for the correct folding of **5** in lanosterol biosynthesis. Such an unusual folding as that shown in **61** and **62** encouraged us to investigate as to how the steric bulk size at the central part of **5** affects the polycyclization pathway. Analogues **65**–**67** having slightly bulky ethyl group(s) (extra C1-unit) at C(10) and/or C(15) were prepared and incubated with pig liver cyclase.[35a–c] Diethylated analogue **65** gave only monocyclic products **68** and **70**. This is the first example of the cyclase reaction being stopped at the stage of the initial A-ring formation,[35a] despite many studies on the substrate analogs having been reported.[1a]

This also definitively demonstrated that the cyclization reaction to protosterol cation **52** proceeds *via* discrete carbocation intermediates, although sometimes this reaction has been assumed to be concerted. Monoethylated **66**, substituted at the 15-position, afforded 6,6,5-fused tricyclic **71** and fully cyclized lanosterol homologue **73**.[35b] Compound **71** could be produced by the deprotonation from the ethyl group at the 14-position of the 6,6,5-fused tricyclic cation (**51** with Et at C-14), which had been produced by Markovnikov closure as shown in Scheme 4. Concomitant production of **71** and **73** indicated that a common intermediate of ethylated **51** could be produced and further verified that **73** could be formed *via* the ring expansion process from ethylated **51**, followed by a series of 1,2-shift rearrangements of hydride and ethyl groups in an anti-parallel manner (Scheme 4). Analogue **67** having an ethyl residue only at C(10) afforded two monocycles **69** and **75**, tricyclic **72** and lanosterol homologue **74**.[35c] Concomitant production of **72** and **74** also gave additional evidence for 5-membered C-ring intermediate **51**. Thus, the idea is now generally accepted that the thermodynamically preferred Markovnikov adduct is formed prior to the ring expansion and further cyclization. Computational studies support the feasibility of such a ring expansion process.[23] Successful trapping of carbocation intermediates is possibly due to the perturbation of a tight binding of the substrate analogues with the lanosterol synthase. Of particular interest is that **75** having the trimethylcyclohexanone moiety was produced *via* twist–boat form **76** by the cyclization of (3*R*)-2,3-oxidodsqualene (Scheme 6, bottom part). Formation of **75**

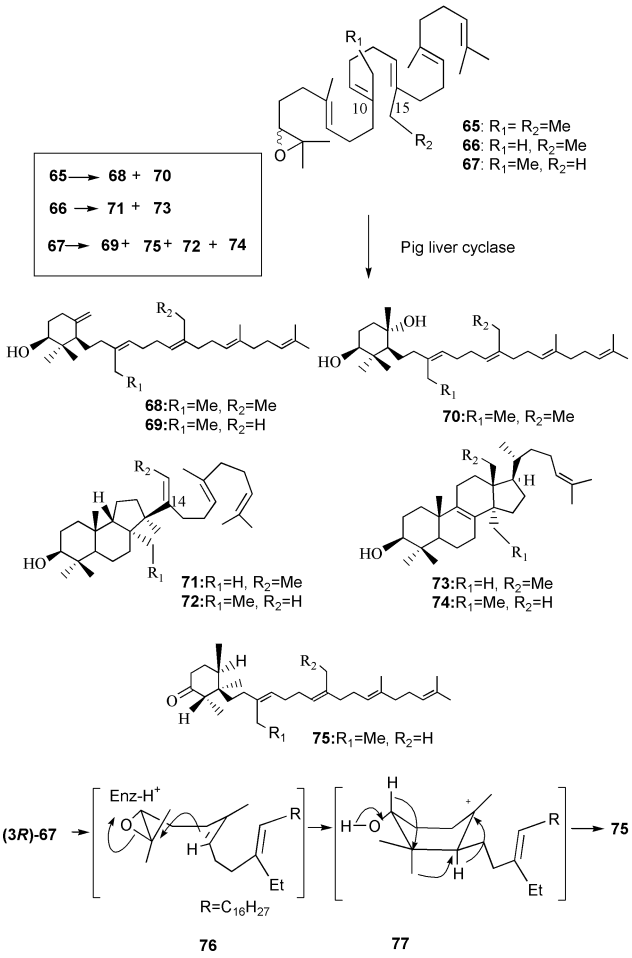

Scheme 6 Cyclization products of oxidosqualene analogues having the slightly bulky ethyl groups at the central part of the substrates.

led to a surprising question, because lanosterol synthase is believed to be active only with (3*S*)-**5**, but inert to (3*R*)-**5**. One possible explanation of this paradox may be that the larger steric bulk size of the ethyl group may have induced incorrect placement of the (3*R*)-epoxide at the catalytic site intrinsic to the (3*S*)-epoxide, where (3*R*)-**67** had been constrained to fold with a boat form **76** in the enzyme cavity and underwent a 1,2-shift of the hydride and methyl group as shown in **77**. Despite the looser binding occurring around the A/B-ring formation site, the cyclase still had binding ability for (3*S*)-**67** which enabled it to form the chair structure, leading to the production of **69** and to further cyclization to form **72** and **74**; the yield (31%) of **69**, **72** and **74** from (3*S*)-**67** was higher than that (7.7%) of **75** from (3*R*)-**67**. Replacements at the central part of **5** with functional groups having different steric bulk sizes (small hydrogen or large ethyl group) afforded different cyclization products (compare Scheme 5 with 6), indicating that an appropriate steric bulk size at the central part of **5** determines the correct folding of **5** leading to completion of the normal polycyclization reaction. The formation of monocyclic **75** and achilleol A[15] homologue **69** was observed from **67**, but not from **66**, indicating that the steric bulk size at C(10) had a greater influence on the polycyclization compared to that at C(15), although the significance of the bulk size at C(15) also is not negligible.

The squalene cyclase from *Tetrahymena pyriformis* (STC) catalyzes the conversion reaction of squalene **1** into 6,6,6,6,6-fused pentacyclic tetrahymanol **78** (Scheme 7). This

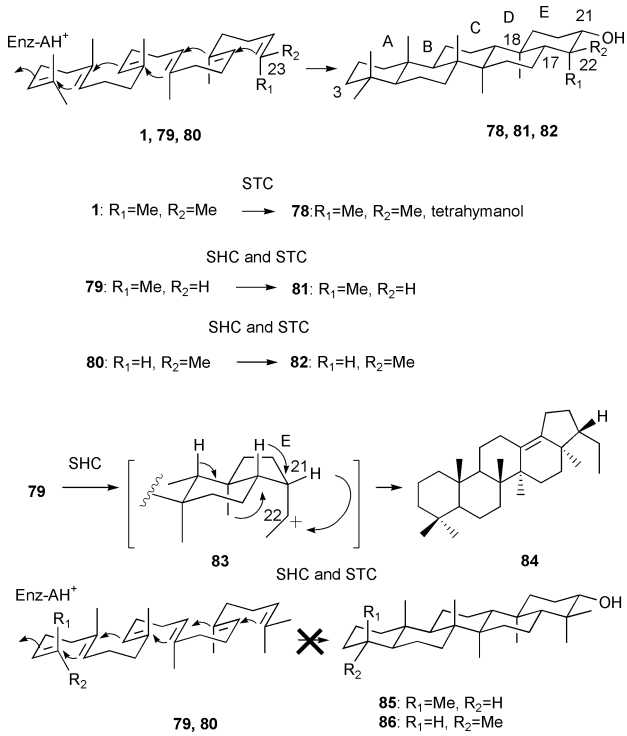

Scheme 7 Effect of the terminal methyl group on the polycyclization reactions by squalene–hopene (SHC) and squalene–tetrahymanol cyclases (STC).

cyclase can also accept (3*R*)- and (3*S*)-**5** as the substrate, giving 3α- and 3β-hydroxytetrahymanol, respectively. Previously, it was reported that **75** was also formed by incubating (3*R*)-**5** with the STC.[36] It is quite interesting from the aspect of molecular evolution that the same trimethylcyclohexanone skeleton is constructed by both protozoa and mammalian cyclases, further supporting the idea that triterpenoid cyclases should have evolved from a common ancestor cyclase.[4]

Substrate recognition by hopene synthase

To gain better understanding of the substrate recognition, some analogues have been synthesized as alternative substrates for SHC and it has been examined whether or not they are the substrates (or inhibitors in some cases).

The structure of hopene **2** differs from that of tetrahymanol **78** only in the terminal E-ring; the 5-membered E-ring for **2**, but the 6-membered one for **78**. The separate incubations of analogue 23-desmethylsqualenes **79** and **80**, lacking one of the two terminal methyl groups, using the native SHC, gave unprecedented cyclization products **81** and **82**, respectively, having a 6,6,6,6,6-fused pentacyclic tetrahymanol skeleton (Scheme 7).[37] As expected, **81** and **82** were also produced, respectively, by separately incubating **79** and **80** with the STC.[37] The E-ring formation proceeds with a complete stereoselectivity; the (23*Z*)-methyl group of **79** was of axial-orientation, while the corresponding *E*-methyl of **79** was arranged to be of equatorial disposition for the E-ring formation. These methyl-orientations of **81** and **82** agree with those inferred from natual deuterated **1** by the STC.[38] The hydroxy groups of **81** and **82** were introduced into the same equatorial disposition as a result of nucleophilic attack of a water molecule in an equatorial direction on the C-21 cation. The cyclization of the 6-membered E-ring formation would be a concerted reaction under stereoelectronic control.[37] The formation of the tetrahymanol skeleton by the SHC, but lacking a C1-unit, is quite interesting from the aspect of molecular evolution. However, the STC has not been cloned and sequenced, thus the amino acid alignment has remained unclear. Only from **79** having the (23*Z*)-methyl group, not from **80**, was neohopane skeleton **84** produced *via* **83** in a series of 1,2-shifts of hydride and methyl groups (Scheme 7), implying that the binding force of the *Z*-methyl to the SHC would be stronger than that of the corresponding *E*-methyl. The final deprotonation reaction from **4** to **2** has been verified to be from the *Z*-methyl group, not from the *E*-methyl group, using deuterated **1** (Scheme 2).[39a]

Compounds **85** and **86** were not found in the incubation mixtures, indicating that the two terminal methyl groups are indispensable for the initiation of the polycyclization reaction. This may be explained as follows. When one of the two terminal methyl groups is missing, the binding force for the isopyropylidene moiety of **1** becomes looser, leading to the incorrect positioning of the terminal ethylidene moiety of **79** and **80**. Thus, the double bond of the ethylidene moiety could not be activated by the attack of a proton, supplied from the DXDDTA motif. However, **79** and **80** still have an isopropylidene moiety at the alternative terminal, which in turn can be tightly captured by the isopropylidene-binding site(s) to start the polycyclization reaction, yielding **81** and **82**. Why were the tetrahymanol-like **81** and **82** produced? The alternative methyl-binding site, positioned at the opposite side to the initiation site, is also likely to be involved in the SHC to facilitate the formation of the desired geometry of **38**, yielding the final product **2**. A lack of the methyl group may have led to a poorer binding and, thus, the 6-membered E-ring may be formed under stereoelectronic control. The *Z*-methyl group binds more strongly with the binding site, compared to the corresponding *E*-methyl group, as exemplified by the production of **84** from **79**.

Incubations of squalene analogs of 6-, 19-, and 15-desmethylsqualenes afforded normal cyclization products having 6,6,6,6,5-fused pentacyclic hopane skeletons.[39b] However, 10-desmethylsqualene gave two unprecedented cyclization products having tetracyclic 6,5 + 5,5 and pentacyclic 6,5 + 5,5 + 6 ring systems.[39b] Therefore, an appropriate bulk size at C(10) of **1** is crucial for the correct folding which directs the normal polycyclization pathway, which is in good agreement with the inference from the OSC. It can be concluded that the following three sites are crucial for the construction of the hopane skeleton: the initiation site, the central site at C(10) and the termination site. The methyl-binding sites must have an accurate steric size to allow a precise interdigitation of each methyl group with each separate binding site.

(3*R*)- and (3*S*)-**5** can also be converted into 3α- and 3β-hydroxyhopene by the SHC, respectively. Prestwich and coworkers reported the enzyme reactions of substrate analogues having a fluorine atom at the central part of **1** (**87** and **90**); the polycyclization reaction terminated at the monocyclic and/or the bicyclic ring stage (Scheme 8).[40] It is likely that bridged

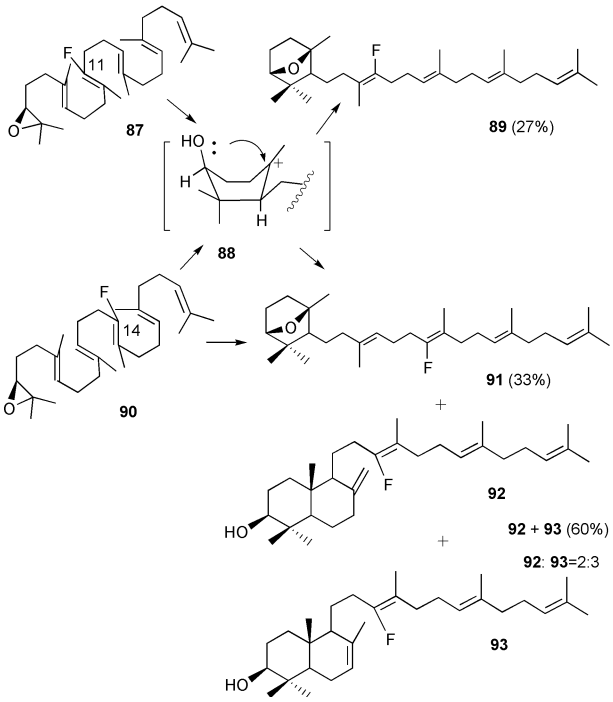

Scheme 8 Cyclization products of 11- and 14-fluoro-(3*S*)-2,3-oxidosqualenes by the native SHC.

bicyclic ethers **89** and **91** were produced *via* twist–boat form **88**. **87** gave only monocyclic **89** in a yield of 27%, whereas **90** afforded mono- **91** and bicyclic **92** and **93** in yields of 33% and 60% (**92**:**93** = 2:3), respectively. This may be explained in terms of the electronic and/or steric perturbation induced by the fluorine atom. Introduction of a fluorine atom at C(11) decreased the π-electron density of the double bond at 10- and 11-positions due to the electron-withdrawing function. This may have led to the failure of nucleophilic attack of the double bond to the C10-cation of **33** required for the formation of bicyclic intermediate **34**, thus ending in monocyclic **89**. The larger fluorine atom may have induced boat form **88** in the enzyme cavity, as found in the case of **67**. Poorer electron density of the double bond at 14 and 15 positions, which was induced by the introduction of a fluorine at C(14), decreased the nucleophilic reactivity, leading to the termination of polycyclization reaction at the bicyclic reaction stage **34** (**92** and **93**) without occurrence of the subsequent cyclization. In addition, the larger steric bulk size of a fluorine atom may have perturbed the optimal folding conformation, resulting in quenching the polycyclization reaction at the monocyclic ring stage **33** (**91**).

Scheme 9 shows the enzymic products of 18(*Z*)-(3*S*)-29-methylidene-2,3-oxidosqualene **94** (29-MOS) [41a] and its geometrical *E*-isomer **96**[41b] by the native SHC. Compound **94** is reported as the mechanism-based irreversible inhibitor (a suicide substrate) for OSCs.[12,42] The pentacyclic **95** having a 6,6,6,5 + 6 ring system was also trapped from **94** and **96**, further supporting that intermediate **37** having 17β-H is involved and that formation of **95** proceeds in such a conformation as depicted in the bottom of Scheme 9 (see also **46**). **94** gave only pentacyclic **95**, but the isolated yield was very small (2.75%).[41a] On the other hand, **96** gave bicyclic **97** and **98**, quenched at the earlier reaction stage, in a high yield (25%) and **95** in a 2.5% yield.[41b] The total conversion ratio from **96** was considerably higher than that of **94**. The lower isolation yield of **95** from **94** may imply that a large amount of 17-*epi*-dammarenyl cation intermediate (**35** with a methylidene residue), which was produced during the cyclization, may have been used for

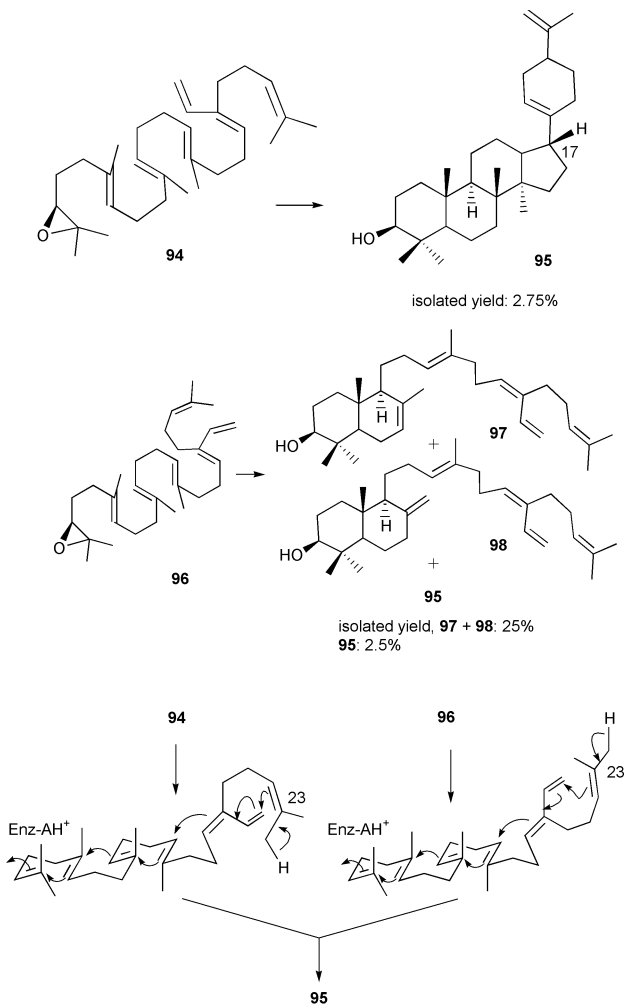

Scheme 9 Cyclization products of 18(*Z*)- and 18(*E*)-29-methylidene-2,3-oxidosqualenes by the SHC.

Table 2 Sulfur-substituted oxidosqualene analogues as inhibitors of *A. acidocaldarius* SHC.[44a]

Compds.	IC_{50}/nM	K_I/nM	k_{inact}/ min^{-1}
99 S-6	150	127	0.0001
100 S-10	570	971	0.0001
101 S-14	86	109	0.054
102 S-18	60	31	0.071
103 S-19	78	83	0.054
94 29-MOS	1200	2100	0.06

covalent modification of the SHC (Table 2). However, **96** can also bind to the SHC through the formation of a covalent bond.[41b] Why did **96** have a higher conversion ratio and give a larger amount of bicyclic **97** and **98**, compared to **94**, despite both **94** and **96** having been employed for covalent binding with the SHC? Further investigations are necessary to address this question.

Acyclic, mono-, bi- and tricyclic compounds, which possess nitrogen atoms at positions of the transient carbocation formed during the polycyclization process, have been shown to inhibit OSC activities.[1a,43] Fig. 4 shows potent inhibitors containing a sulfur atom against the SHC,[44a] and the inhibition activities are shown in Table 2. These sulfur-substituted squalene oxide analogues were also effective against OSCs.[44b] The inhibition mechanism is similar to that of aza-squalene oxide analogues; during the polycyclization progress, the sulfur atom is changed to the positively charged sulfonium ion, which can mimic the carbocation intermediates shown in Scheme 2. **99** and **100**

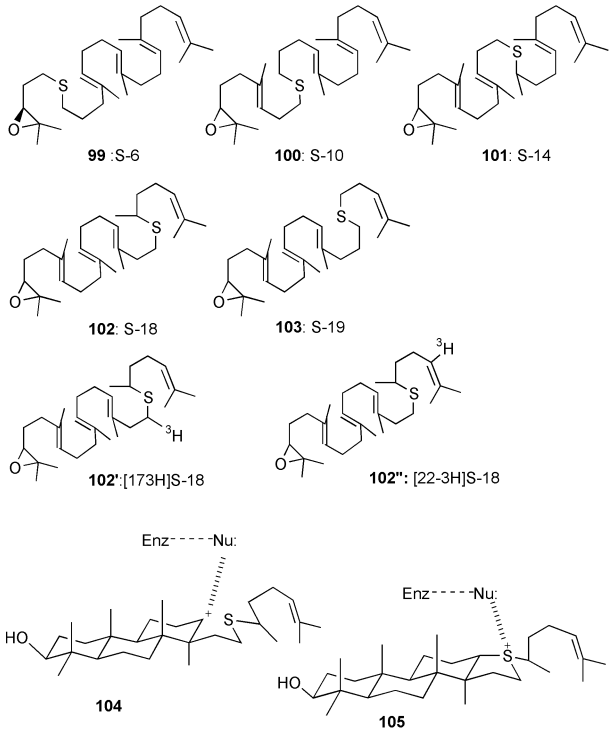

Fig. 4 Structures of sulfur-substituted oxidosqualene analogues and inhibition mechanism.

showed no time dependency, thus, they act only as a substrate mimic. On the other hand, **101**–**103** were time-dependent inhibitors, **102** being the most potent inhibitor to date. Each native SHC was radiolabeled by incubating both **102′** and **102″**, suggesting the irreversible adduct formation or the covalent modification of the active sites. Tri- and tetracyclic **104** and **105** have been proposed as the adduct structures.[44a]

Summary

As represented by products **10**, **12**, **26** and **27**, site-directed mutagenesis not only helps to understand the fundamental issue of the reaction mechanism (molecular recognition and catalytic function) but also generates previously unknown unnatural natural products. The rational genetic engineering of the active and/or recognition sites is a promising tool for the creation of novel natural products and new drugs. A variety of triterpene skeletons could be created by subtle changes in the active sites. Steric bulk size of the active components would be one of the major factors for precise enzymatic control leading to a structural diversity of triterpenes. This idea may also be supported by the finding that methyl-deficient or slightly bulky substrates gave dramatically altered products as shown in Schemes 5–9. Thus, a combination of mutagenesis and slightly modified substrates would lead to further creation of previously unknown terpene skeletons. From the aspect of molecular evolution, it is noteworthy that the mutations of cycloartenol and lupeol synthases led to the formation of lanosterol and β-amyrin, respectively, as a major product.[45a,b] Recently, very interesting reports have appeared that multiple triterpenes (up to 6 or 9) were produced by a single triterpene synthase from *Arabidopsis thaliana*.[8b,46] The native *A. acidocaldarius* SHC also affords several products: **2** (*ca.* 80%), **3** (*ca.* 20%), five tetracyclic products **19**–**23** in a small amount (< 1%) and one pentacyclic product **30** (< 1%).[22c] Many triterpenes are also included in almost equivalent amounts in the *Zymomonas mobilis* cells;[47] probably the single SHC enzyme may be responsible for the multiple production. The deep insight into *Z. mobilis* SHC may further lead to the well-defined understanding of squalene cyclases. The structural diversity of triterpene

skeletons obtained by a single enzyme implicates that a dedicated cyclase for all triterpene skeletons may be unnecessary; that is, some triterpene skeletons could be minor products of other triterpene synthases.[46]

Acknowledgements

I (T. H.) thank the young scientists who have made great contributions to this research; their names are included in the literature. Financial support has been provided by the Ministry of Education, Science and Culture of Japan and by the Fujisawa Foundation. I sincerely appreciate Professor A. I. Scott, who guided this interesting field outlined here.

Notes and references

1 (*a*) I. Abe, M. Rohmer and G. D. Prestwich, *Chem. Rev*., 1993, **93**, 2189; (*b*) K. U. Wendt, G. E. Schulz, E. J. Corey and D. R. Liu, *Angew. Chem., Int. Ed., Engl*., 2000, **39**, 2812.
2 B. Seckler and K. Poralla, *Biochem. Biophys. Acta*., 1986, **881**, 356.
3 D. Ochs, C. Kaletta, K.-D. Entian, A. Beck-Sickinger and K. Poralla, *J. Bacteriol*., 1992, **174**, 298.
4 (*a*) M. Rohmer, P. Bouvier and G. Ourisson, *Proc. Natl. Acad. Sci. USA*, 1979, **76**, 847; (*b*) G. Ourisson, *Pure Appl. Chem*., 1989, **61**, 345.
5 A. Tippelt, L. Jahnke and K. Poralla, *Biochem. Biophys. Acta*, 1998, **1391**, 223 and refs. cited therein.
6 C. J. Buntel and J. H. Griffin, *J. Am. Chem. Soc*., 1992, **114**, 9711.
7 S. M. Godzina, M. A. Lovato, M. M. Meyer, K. A. Foster, W. K. Wilson, W. Gu, E. L. de Hostos and S. P. T. Matsuda, *Lipids*, 2000, **35**, 249 and refs. cited therein.
8 (*a*) M. Morita, M. Shibuya, T. Kushiro, K. Masuda and Y. Ebizuka, *Eur. J. Biochem*., 2000, **267**, 3453; (*b*) T. Kushiro, M. M. Shibuya, K. Masuda and Y. Ebizuka, *Tetrahedron Lett*., 2000, **41**, 7705 and refs. cited therein.
9 T. Sato, Y. Kanai and T. Hoshino, *Biosci. Biotechnol. Biochem*., 1998, **62**, 407.
10 (*a*) K. U. Wendt, K. Poralla and G. E. Schulz, *Science*, 1997, **277**, 1811; (*b*) K. U. Wendt, A. Lenhart and G. E. Schulz, *J. Mol. Biol*., 1999, **286**, 175.
11 C. Feil, R. Sussmuth, G. Jung and K. Poralla, *Eur. J. Biochem*., 1996, **242**, 51.
12 I. Abe and G. D. Prestwich, *J. Biol. Chem*., 1994, **269**, 802.
13 E. J. Corey, H. Cheng, C. H. Baker, S. P. T. Matsuda, D. Li and X. Song, *J. Am. Chem. Soc*., 1997, **119**, 1289.
14 (*a*) T. Sato and T. Hoshino, *Biosci. Biotechnol. Biochem*., 1999, **63**, 2189; (*b*) T. Merkofer, C. Pale-Gosdemange, K. U. Wendt, M. Rohmer and K. Poralla, *Tetrahedron Lett*., 1999, **40**, 2121; (*c*) T. Dang and G. D. Prestwich, *Chem. Biol*., 2000, **7**, 643.
15 A. F. Barrero, E. J. Alvarez-Manzaneda and R. Alvarez-Manzaneda, *Tetrahedron Lett*., 1989, **30**, 3351.
16 W. S. Johnson, S. D. Lindell and J. Steele, *J. Am. Chem. Soc*., 1987, **109**, 5852.
17 D. A. Dougherty, *Science*, 1996, **271**, 163.
18 K. Poralla, *Bioorg. Med. Chem. Lett*., 1994, **4**, 285.
19 T. Sato and T. Hoshino, *Biosci. Biotechnol. Biochem*., 1999, **63**, 1171.
20 T. Sato and T. Hoshino, *Biosci. Biotechnol. Biochem*., 2001, **65**, 2233.
21 T. Hoshino and T. Sato, *Chem. Commun*., 1999, 2005.
22 (*a*) T. Sato, T. Abe and T. Hoshino, *Chem. Commun*., 1998, 2617; (*b*) T. Hoshino, M. Kouda, T. Abe and S. Ohashi, *Biosci. Biotechnol. Biochem*., 1999, **63**, 2038; (*c*) C. Pale-Gosdemange, C. Feil, M. Rohmer and K. Poralla, *Angew. Chem., Int. Ed. Engl*., 1998, **37**, 2237.
23 C. Jenson and W. L. Jorgensen, *J. Am. Chem. Soc*., 1997, **119**, 10846.
24 T. Abe and T. Hoshino, to be published, presented at 44th Symposium on the Chemistry of Terpenes, Essential Oils, and Aromatics, Sapporo in 2000. Symposium paper pp. 129–131.
25 T. Hoshino, M. Kouda, T. Abe and T. Sato, *Chem. Commun*., 2000, 1485.
26 (*a*) C. Pale-Grosdemange, T. Merkofer, M. Rohmer and K. Poralla, *Tetrahedron Lett*., 1999, **40**, 6009; (*b*) C. Füll and K. Poralla, *FEMS Microbiol. Lett*., 2000, **183**, 221; (*c*) S. Schmitz, C. Füll, T. Glaser, K. Albert and K. Poralla, *Tetrahedron Lett*., 2001, **42**, 883.
27 T. Hoshino, T. Abe and M. Kouda, *Chem. Commun*., 2000, 441.
28 F. Viola, M. Ceruti, L. Cattel, P. Milla, K. Poralla and G. Balliano, *Lipids*, 2000, **35**, 297.
29 T. Sato, S. Sasahara, T. Yamakami and T. Hoshino, submitted for publication.
30 (*a*) B. M. Joubert, L. Hua and S. P. T. Matsuda, *Org. Lett*., 2000, **2**, 339; (*b*) S. P. T. Matsuda, L. B. D. Darr, A. H. Hart, J. B. R. Herrera, K. E. McCane, M. M. Meyer, J. Pang and H. G. Schepmann, *Org. Lett*., 2000, **2**, 2261.
31 (*a*) E. J. Corey and H. Cheng, *Tetrahedron Lett*., 1996, **37**, 2709; (*b*) E. J. Corey, S. C. Virgil, H. Cheng, C. H. Baker, S. P. T. Matsuda, V. Singh and S. Sarshar, *J. Am. Chem. Soc*., 1995, **117**, 11819.
32 (*a*) A. Krief, J. R. Scauder, E. Guittet, C. Herve du Penhoat and J. Y. Lallemand, *J. Am. Chem. Soc*., 1987, **109**, 7910; (*b*) A. Krief, P. Pasau and L. Quéré, *Bioorg. Med. Chem. Lett*., 1991, **1**, 365; (*c*) A. Krief, P. Pasau, E. Guittet, Y. Y. Shan and M. Herin, *Bioorg. Med. Chem. Lett*., 1993, **3**, 365.
33 E. J. Corey, S. C. Virgil, D. R. Liu and S. Sarsha, *J. Am. Chem. Soc*., 1992, **114**, 1524.
34 E. E. van Tamlene, *J. Am. Chem. Soc*., 1968, **90**, 3284.
35 (*a*) T. Hoshino, E. Ishibashi and K. Kaneko, *Chem. Commun*., 1995, 2401; (*b*) T. Hoshino and Y. Sakai, *Chem. Commun*., 1998, 1591; (*c*) T. Hoshino and Y. Sakai, *Tetrahedron Lett*., 2001, **42**, 7319.
36 I. Abe and M. Rohmer, *J. Chem. Soc., Perkin Trans. 1*, 1994, 783.
37 T. Hoshino and T. Kondo, *Chem. Commun*., 1999, 731.
38 (*a*) P. Bouvier, Y. Berger, M. Rohmer and G. Ourisson, *Eur. J. Biochem*., 1980, **112**, 549; (*b*) M. Renoux and M. Rohmer, *Eur. J. Biochem*., 1986, **155**, 125.
39 (*a*) T. Hoshino and T. Kondo, to be published, presented at Annual Meeting of Society for Biosci. Biotechnol. and Agrochem. April, 1998, Nagoya. Abstract p. 256; (*b*) T. Hoshino and S. Ohashi, to be published, presented at 43th Symposium on the Chemistry of Terpenes, Essential Oils, and Aromatics, Ooita in 1999. Symposium paper pp. 229–231.
40 (*a*) B. Robustell, I. Abe and G. D. Prestwich, *Tetrahedron Lett*., 1998, **39**, 957; (*b*) B. Robustell, I. Abe and G. D. Prestwich, *Tetrahedron Lett*., 1998, **39**, 9385.
41 (*a*) I. Abe, T. Dang, Y. F. Zheng, B. A. Madden, C. Feil, K. Poralla and G. D. Prestwich, *J. Am. Chem. Soc*., 1997, **119**, 11333; (*b*) Y. F. Zheng, I. Abe and G. D. Prestwich, *J. Org. Chem*., 1998, **63**, 4872.
42 (*a*) X.-y. Xiao and G. D. Prestwich, *J. Am. Chem. Soc*., 1991, **113**, 9673; (*b*) I. Abe, M. Bai, X.-y. Xiao and G. D. Prestwich, *Biochem. Biophys. Res. Commun*., 1992, **187**, 32.
43 T. Hoshino, N. Kobayashi, E. Ishibashi and S. Hashimoto, *Biosci. Biotechnol. Biochem*., 1995, **59**, 602.
44 (*a*) Y. F. Zheng, I. Abe and G. D. Prestwich, *Biochemistry*, 1998, **37**, 5981; (*b*) D. Stach, Y. F. Zheng, A. L. Perez, A. C. Oehlschlager, I. Abe, G. D. Prestwich and P. G. Hartman, *J. Med. Chem*., 1997, **40**, 201.
45 (*a*) J. B. R. Herrera, W. K. Wilson and S. P. T. Matsuda, *J. Am. Chem. Soc*., 2000, **122**, 6765; (*b*) T. Kushiro, M. Shibuya, K. Masuda and Y. Ebizuka, *J. Am. Chem. Soc*., 2000, **122**, 6816.
46 M. J. R. Segura, M. M. Meyer and S. P. T. Matsuda, *Org. Lett*., 2000, **2**, 2257.
47 E. Douka, A. Koukkou, C. Drainas, C. Grosdemange-Billiard and M. Rohmer., *FEMS Microbiol. Lett*., 2001, **199**, 247.